

THERMOLUMINESCENT RELAXATION OF STABLE SYSTEMS

W.F. HORNYAK, Reuven CHEN * and Alan FRANKLIN

University of Maryland, Archaeometric Laboratory College Park, MA 20742, USA

Received 2 October 1989

Accepted 26 December 1989

The Kohlrausch relaxation function (or the stretched exponential function) is compared in detail with a kinetic model for isothermal temperature stimulated luminescent decay based on a Gaussian distribution of activation energies. In each case the reactivity rate is assumed to follow an Arrhenius form (or the Randall–Wilkins form) $s \exp(-E/kT)$. Use of the Gaussian distribution has been found to give a good accounting of observed experimental results. The present investigation is primarily meant to determine the uniqueness of such fits to experimental data. As appropriate for this purpose, the controlling parameters of the two relaxation functions are forced into equivalence by an imposed normalization. The normalization point is selected for a critical time to best reveal the differences between the two time dependent relaxation functions. Although the resulting two decay functions are not rendered completely identical, close numerical agreement over a wide range of relaxation times and activation energy distribution widths is found. The similarity in the widths of the corresponding energy distributions is found to be the main reason for this close agreement. Exact features of the activation energy distribution are important only in the very short and very long time periods of the relaxation process. Recovering the activation energy distribution from experimentally measured data is discussed in detail.

1. Introduction

The ubiquitous stretched exponential relaxation decay law introduced by R. Kohlrausch (1854) [1] and F. Kohlrausch (1863) [2] has by now been found to fit a vast number of relaxation problems [3]. A number of investigators have considered a variety of physical models that would lead to the stretched exponential law or closely related random walk relationships [4–7]. The strong suggestion exists that the stretched exponential law may operate in the case of isothermal temperature stimulated luminescence (TSL or simply TL) relaxation.

TL relaxation processes often involve multiple decay mechanisms operating simultaneously. In order to narrow possibilities to a single process only materials that involve trap sites that are

stable at room temperature and have been allowed to complete any low temperature fading that might be present by long term storage are considered [8,9]. The isothermal relaxation of such materials at an elevated temperature is expected to proceed with de-trapping through the conduction band. In addition the clearest conclusions would be derived for materials showing a single isolated glow curve peak upon heating at an increasingly elevated temperature.

Very few TL phosphor materials of the above type have been studied in isothermal relaxation. TLD 400 (CaF₂:Mn) ribbon phosphor material shows a single well isolated temperature–wavelength peak in a 3D-spectrophotometric display [10]. The paucity of data on such phosphor materials precludes a thorough experimental test of the stretched exponential decay law in TL. However, a closed form theoretical expression has been derived that very successfully fits observed data and gives consistent physical parameters for both glow curve data and isothermal decay for TLD 400 [11]. This suggests the strategy of com-

* Permanent address: School of Physics and Astronomy, Raymond and Beverly Sackler Faculty of Exact Sciences, Tel Aviv University, Tel Aviv 69978, Israel.

paring this theoretical model relaxation function with the stretched exponential law. Such a comparison will have bearing on the possible uniqueness of the derived activation energy distributions derived from the data.

2. TL relaxation functions

To account for relaxation phenomena some donor species is invoked that undergoes decay so that the concentration of donors decreases with elapsed time. The stretched exponential function relates to the probability that, at time t , a donor has not yet undergone decay. In the case of the thermoluminescence process undergoing isothermal decay the donors may properly be identified as the electrons occupying trap sites in the material. It is primarily their reduction in number with increasing time that produces the observed thermoluminescent light output. Thus the stretched exponential function takes the form:

$$n = n_0 \exp - (t/\tau_0)^\xi, \quad (1)$$

where n and n_0 refers to the number of trapped electrons per cm^3 at time t and time $t = 0$, respectively.

For the suggested comparison, a simple first order kinetic model with a Gaussian activation energy distribution at $t = 0$ is used. Electrons trapped at a single type of site are elevated to the conduction band from which they rapidly react with holes at recombination sites, emitting the observed TL light. No re-trapping is allowed. A distribution of activation energies $\rho(E)$ for the electron trap sites is assumed to be the Gaussian:

$$\rho(E) = N \sqrt{\frac{a}{\pi}} \exp - a(E - E_0)^2. \quad (2)$$

The trapped electron distribution as a function of energy and time is written:

$$\eta(E, t) = f(E, t)\rho(E) \quad (3)$$

by introducing the electron occupation number $f(E, t)$. The total number of trapped electrons at time t is:

$$n = n(t) = \int_0^\infty f(E, t)\rho(E) dE. \quad (4)$$

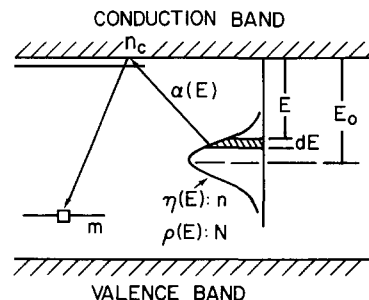


Fig. 1. A simple kinetic model for TL showing an electron trap activation energy distribution $\rho(E)$ and an electron occupation density $\eta(E)$. The density of holes at the recombination site is labelled m .

The density of holes at the single recombination type centers is m . Electrons in a narrow energy band dE at energy E are elevated into the conduction band at a rate:

$$\alpha = s \exp(-E/kT), \quad (5)$$

where s is the frequency factor, k is the Boltzmann constant, and T the isothermal absolute temperature. Figure 1 shows the kinetic model described.

At $t = 0$ the electron distribution is taken to be directly proportional to $\rho(E)$ or $\eta(E, 0) = f_0\rho(E)$. This assumption of proportionality is expected to be valid if the trapped electrons resulted from a laboratory irradiation using beta or gamma rays, as is commonly the case in TL studies. This assumption is also not implausible even if the exciting irradiation makes use of low energy photons provided the irradiation is of short enough duration to prevent an excessive population of deeper trap sites through the ongoing competition in the photo-excitation-de-excitation process [12].

The intensity of the emitted TL light is proportional to dm/dt , the rate of decrease in the hole concentration at the recombination centers. If the usual assumptions are made concerning the concentration of electrons n_c in the conduction band, that n_c and dn_c/dt are both negligibly small, it follows that $m = n$ and $dm/dt = dn/dt$. These assumptions are also implied by writing n instead of m in eq. (1). These same assumptions for the model under discussion yields:

$$\frac{dn}{dt} = \frac{\alpha_0 n_0}{\sqrt{\pi}} yG(x, y) \equiv -\alpha_0 n_0 H(x, y), \quad (6)$$

where α_0 is α of eq. (5) with $E = E_0$, $x = \alpha_0 t$, and $y^2 = ak^2 T^2$ with a the constant appearing in eq. (2). The function $G(x, y)$ is the so-called "after effect function" introduced by Wagner [13] and tabulated in Jahnke and Emde [14]. Equation (6) is derived in ref. [11].

The Gaussian distribution given by eq. (2) is an ad hoc assumption. Stochastic processes might be imagined to play a significant role both in the formation of the trap sites as well as in the subsequent trapping of electrons in the initial irradiation phase [15]. Conditions may therefore be present leading to an initial electron population distribution possibly better described by the stretched exponential law.

For the stretched exponential function of eq. (1) the time derivative provides the analog to eq. (6):

$$\frac{dn}{dt} = -\frac{n_0 \zeta}{\tau_0} \left(\frac{t}{\tau_0}\right)^{\zeta-1} \exp - (t/\tau_0)^\zeta. \quad (7)$$

In order to compare the Gaussian distribution model to that based on the stretched exponential model it is necessary to establish a correspondence between eqs. (6) and (7). The limiting cases for large and small values of the parameters y in eq. (6) and ζ in eq. (7) are examined for this purpose.

In view of the definition of y and eq. (2) $y \ll 1$ corresponds to a very broad distribution $\rho(E)$ while $y \gg 1$ corresponds to a very narrow distribution. It is easy to show that

$$\lim_{y \rightarrow 0} G(x, y) = 1/x, \quad (8)$$

whence for $y \ll 1$

$$\frac{dn}{dt} = -\frac{n_0}{\sqrt{\pi}} y t^{-1} = -\text{constant} \cdot t^{-1}. \quad (9)$$

Such an inverse time dependence is frequently observed experimentally.

On the other hand it is also easy to show that

$$\lim_{y \rightarrow \infty} \left[\frac{yG}{\sqrt{\pi}}(x, y) \right] = e^{-\alpha_0 t}, \quad (10)$$

whence

$$dn/dt = -\alpha_0 n_0 e^{-\alpha_0 t} = -I_0 e^{-\alpha_0 t}, \quad (11)$$

the appropriate exponential decay for a very narrow distribution $\rho(E)$. This type of decay ex-

PLICITLY exhibits simple first order kinetics with a constant decay rate since $dn/dt = -\alpha_0 n$.

For the stretched exponential function of eq. (2), when $\zeta \ll 1$ and t/τ_0 is not exactly zero $(t/\tau_0)^\zeta = 1$, hence

$$dn/dt = -\frac{n_0 \zeta}{e} \cdot t^{-1} = -\text{constant} \cdot t^{-1}, \quad (12)$$

leading again to an inverse time dependence. To achieve the t^{-1} dependence ζ need not be very small. Indeed for $\zeta = 0.1$ a very close t^{-1} behavior results for an entire range $0.01 < t/\tau_0 < 25$.

On the other hand, when $\zeta = 1$ eq. (7) reduces to

$$\frac{dn}{dt} = -\frac{n_0}{\tau_0} e^{-t/\tau_0} = -I_0 e^{-t/\tau_0}. \quad (13)$$

To obtain an exponential behavior obeying eq. (13) from $t = 0$ to beyond $t/\tau_0 = 10$ requires $\zeta > 0.99$. For example, if $\zeta = 0.95$ the actual behavior in this range of t/τ_0 begins to deviate appreciably from the exponential law given by eq. (13).

Comparison of eq. (12) to eq. (9) and eq. (13) to eq. (11) carries the suggestion that the two functions:

$$H(x, y) = \frac{yG(x, y)}{\sqrt{\pi}} \quad \text{and} \quad (14)$$

$$F(t/\tau_0, \zeta) = \zeta (t/\tau_0)^{\zeta-1} \exp - (t/\tau_0)^\zeta,$$

might be closely related if $x = \alpha_0 t$ is taken equal to $x = t/\tau_0$. An identification often adopted in using the stretched exponential is in fact

$$\tau_0^{-1} = s \exp(-E_0/kT) = \alpha_0.$$

It remains to establish the relationship between y and ζ , and to test the extent of the equivalence as a function of x .

To relate y and ζ the two functions in eq. (14) are equated for some most revealing choice of x , finding for selected values of ζ the corresponding value of y . The two functions of eq. (14) show the greatest variation with y or ζ when $x \approx 1$, therefore $x = 1$ is selected for the normalization of the two functions. This normalization should produce the most stringent test for the equivalence of $H(x, y)$ and $F(x, \zeta)$, additional significance for this choice of normalization will be given later. The results are given in table 1 under the column

Table 1
Relationship between the parameters ζ and y

| ζ | y | y' | FWHM (eV) ^{a)} |
|---------|----------|----------|-------------------------|
| 0 | 0 | 0 | 0 |
| 0.05 | 0.033 | 0.030 | 2.18 |
| 0.10 | 0.067 | 0.062 | 1.09 |
| 0.20 | 0.134 | 0.131 | 0.538 |
| 0.30 | 0.21 | 0.21 | 0.34 |
| 0.40 | 0.30 | 0.30 | 0.24 |
| 0.50 | 0.40 | 0.41 | 0.18 |
| 0.60 | 0.54 | 0.54 | 0.13 |
| 0.70 | 0.70 | 0.71 | 0.103 |
| 0.80 | 0.95 | 0.95 | 0.076 |
| 0.90 | 1.47 | 1.36 | 0.053 |
| 0.95 | 2.15 | 1.76 | 0.041 |
| 0.99 | - | 2.71 | 0.027 |
| 1 | ∞ | ∞ | 0 |

^{a)} At $T = 230^\circ\text{C} = 503\text{ K}$, based on y' values.

labelled y and plotted in fig. 2. An empirical relationship between y and ζ was found to be:

$$\zeta = 1 - e^{-y/c} \leftrightarrow y = c \ln(1 - \zeta)^{-1}, \quad (15)$$

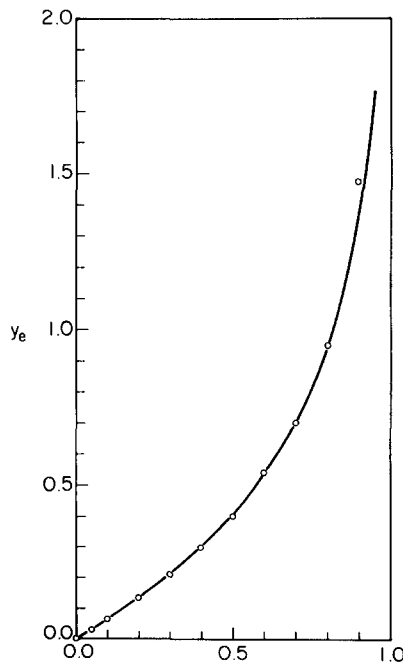


Fig. 2. The equivalent value of y as a function of ζ to achieve normalization of $H(x, y)$ and $F(x, \zeta)$ at $x=1$. The smooth curve is for eq. (15) and the points are for the exact numerical correspondence.

with $c = 0.589$. A comparison set of values y' calculated from eq. (15) is also shown in table 1. It is to be noted that the exact values of y obtained from a numerical fit and y' obtained from eq. (15) agree fairly well in the range $0.10 < \zeta < 0.90$. A value of $c = \sqrt{\pi}/e = 0.652$ obtained by directly comparing eq. (9) and eq. (12) gives a better accounting for both $\zeta < 0.10$ and $\zeta > 0.90$.

For the theory leading to eq. (6) the “full width at half maximum” (FWHM) for the Gaussian distribution is related to y by:

$$\text{FWHM} = \frac{2kT}{y} \sqrt{0.693}. \quad (16)$$

Values of the width FWHM are also shown in table 1 for an assumed typical isothermal temperature of $230^\circ\text{C} = 503\text{ K}$.

Using eq. (15) to relate ζ and y , and taking $x = \alpha_0 t = t/\tau_0$ a comparison was made between the two functions of eq. (14) for various values of y (and therefore ζ) and x . Generally good agreement was found for x in the range $0.1 < x < 10$

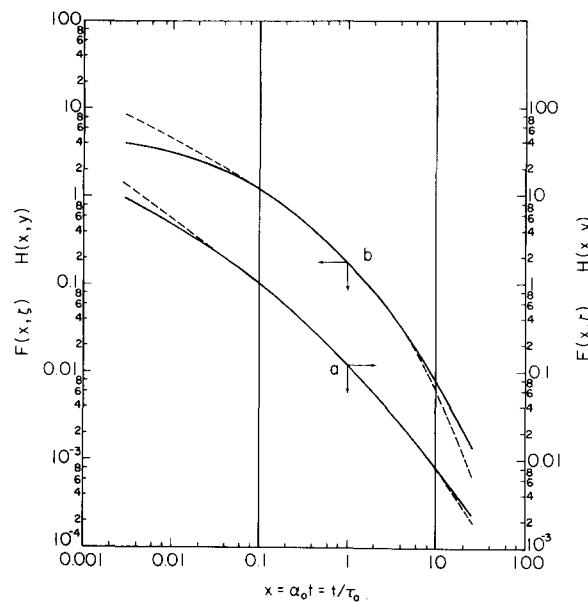


Fig. 3. Comparison of the two decay functions of eq. (14). The solid line curves are for the simple model $H(x, y)$ and the dashed line curves are for the normalized stretched exponent law $F(x = t/\tau_0, \zeta)$. The equivalent parametric values are $\zeta = \frac{1}{3}$ and $y = 0.239$ for the set labelled (a) and $\zeta = \frac{1}{2}$ and $y = 0.40$ for the set labelled (b). The normalization in each case is for $x=1$.

for all values of y . Figure 3 shows the results obtained: (a) for $\zeta = \frac{1}{3}$ (the dashed curve), corresponding to $y = 0.239$ (the solid curve); and (b) for $\zeta = \frac{1}{2}$ (the dashed curve) corresponding to $y = 0.40$ (the solid curve). For these values of ζ the isothermal decay curve shape is in very strong transition from the t^{-1} shape to the simple exponential shape and hence offers a good check on the possible equivalence. There would be very little point in comparing the two relaxation functions for either ζ very close to zero or very close to unity since equivalence for such values is already evident. Figure 3 shows that the agreement for a wide range of values of x is quite good. Failure of agreement over very small and very large values of x will be discussed in the next section.

The universal nature of the time variable in fig. 3 should be noted. Only the quantity $x = \alpha_0 t$ is varied; any combination of s and E_0 is allowed. Once α_0 is determined a particular value of x will correspond to a particular relaxation time.

3. Activation energy distributions

A reactivity distribution function $f(\tau)$ follows from the Laplace transform of the stretched exponential function of eq. (1). If a generalized Arrhenius rate equation

$$\tau^{-1} = s \exp(-E/kT) \quad (17)$$

is adopted a specific activation energy distribution $\phi(E)$ emerges for each value of ζ . Obtaining these energy distributions requires numerical calculations; only for $\zeta = \frac{1}{3}$ and $\zeta = \frac{1}{2}$ are closed form expressions available [3].

A universal representation of the activation energy distributions is possible in terms of the variable $\tau/\tau_0 = (E - E_0)/kT$:

$$f(\tau/\tau_0) \rightarrow \phi(\exp[(E - E_0)/kT]). \quad (18)$$

The distribution function of eq. (18) is thus only a function of $\Delta E = E - E_0$, with the value $\tau/\tau_0 = 1$ corresponding to $E = E_0$. These energy functions are quite asymmetric and possess a long low energy tail. Only in the limit $\zeta = 1$ does the peak of the distribution correspond to $\Delta E = 0$, the true position of E_0 .

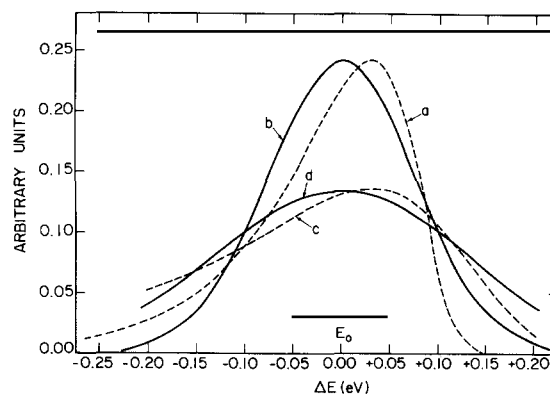


Fig. 4. The activation energy distributions for the equivalent pair $\zeta = \frac{1}{2}$, $y = 0.40$ (a) and (b) respectively and the pair $\zeta = \frac{1}{3}$, $y = 0.239$ (c) and (d). The value of kT used is 0.0433 eV (i.e. for 230 °C). These curves are independent of any particular E_0 that might be assumed.

The Gaussian distribution of activation energies given by eq. (2) is also only a function of $\Delta E = E - E_0$, making the comparison of the two distribution functions particularly convenient. Figure 4 shows the distributions $\phi(\Delta E)$ and $\rho(\Delta E)$ for (a) $\zeta = \frac{1}{2}$, (b) $y = 0.40$, the equivalent y ; (c) $\zeta = \frac{1}{3}$ and (d) $y = 0.239$, the equivalent y . These are the same values used to generate the curves shown in fig. 3.

The main similarity of the two pairs of distribution functions is in the corresponding half widths, (a) with (b) and (c) with (d). In fine detail, curves (a) and (b) in particular seem quite disparate. Why then the close agreement in the relaxation functions shown in fig. 3(b) based on these two distributions?

The isothermal relaxation rate may be expressed in the form:

$$\frac{dn}{dt} = - \int_0^{\infty} \alpha(E) e^{-\alpha(E)t} \eta(E, 0) dE, \quad (19)$$

where $\alpha(E) = s \exp(-E/kT)$. This result follows from eq. (4) with $f(E, t) = f_0 e^{-\alpha(E)t}$ appropriate in the absence of retrapping, and time differentiation under the integral sign. This equation is valid for whatever shape is assumed for $\eta(E, 0)$, the activation energy distribution of the trapped electrons at $t = 0$.

As the isothermal decay process proceeds in time, a window function

$$w(E, t) = \alpha(E) e^{-\alpha(E)t} \quad (20)$$

sweeps through the distribution $\eta(E, 0)$; at each instant of time the relaxation rate is the overlap integral of the window function and the initial distribution of activation energies. The window function has its peak value occur at

$$E_{\max} = kT \ln st \quad (21)$$

and has a width $\text{FWHM} = 2.48kT$ (independent of t). It should be noted that the selection of $x = 1$ leading to eq. (15) corresponds to placing the window function peak at E_0 . The relationship between the position of the window function peak at an energy $E_0 + \Delta E$ in fig. 4 and the corresponding value of x in fig. 3 is:

$$x(E_0 + \Delta E) = e^{\Delta E/kT}. \quad (22)$$

Figure 5 shows the same distribution functions (a) and (b) of fig. 4 for $\zeta = \frac{1}{2}$ and $y = 0.40$. For the latter distribution of $\text{FWHM} = 4.16kT$. In addition the window function $w(E, t)$ is also shown labelled (c). In the region $-0.10 < \Delta E < +0.10$ eV, the window function apparently is sufficiently broad to blur the distinction between the two distributions, and the equality of the two functions shown by curve (b) in fig. 3 mostly reflects the nearly equal width for the corresponding dis-

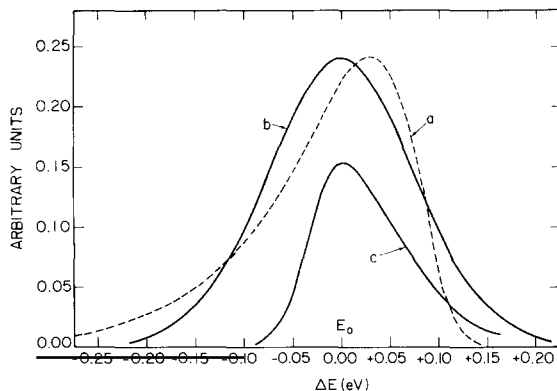


Fig. 5. The same pair of activation energy distributions shown in fig. 4 (a) and (b) and in addition the window function $\alpha e^{-\alpha t}$ at the time $x = 1$ when its peak is at the energy E_0 . The value of kT is 0.0433 eV.

tributions in fig. 5. Applying eq. (22) yields values of $x = 0.1$ and $x = 10$ for $\Delta E = \pm 0.10$ eV. For times corresponding to E less than $(E_0 - 0.10)$ eV the distribution (a) is significantly higher than for (b), thus giving a larger relaxation rate for short times in agreement with fig. 3(b). For times corresponding to E greater than $(E_0 + 0.10)$ eV the opposite is true, with curve (b) significantly higher than (a) again producing results in agreement with fig. 3(b). The same considerations applied to the case $\zeta = \frac{1}{3}$ and $y = 0.239$ clearly suggests close correspondence for the two relaxation functions for a significantly larger range of ΔE . Again this is evident in fig. 3(a).

As pointed out by W. Primak [16], in the event that $\eta(E, 0)$ is sufficiently broader than several kT , eq. (19) may be used to directly determine $\eta(E, 0)$ from the observed relaxation rate. With $\eta(E, 0)$ sufficiently broader than the window function, $\eta(E, 0)$ may be taken outside the integral of eq. (19) giving

$$\frac{dn}{dt} = -\eta(\bar{E}, 0) \int_0^\infty \alpha(E) e^{-\alpha(E)t} dE. \quad (23)$$

The integral in eq. (23) is readily evaluated giving

$$\eta(\bar{E}, 0) = -\frac{t}{kT} \cdot \frac{dn}{dt}. \quad (24)$$

The average energy \bar{E} corresponding to the time t is:

$$\begin{aligned} \bar{E} &= \int_0^\infty E \alpha e^{-\alpha t} dE / \int_0^\infty \alpha e^{-\alpha t} dE \\ &= kT [\ln(st) + 0.5772] \quad \text{when } st \gg 1. \end{aligned} \quad (25)$$

To illustrate this procedure for obtaining $\eta(E, 0)$ from the observed relaxation rate directly, the isothermal decay curve generated for the Gaussian distribution of activation energies with $\text{FWHM} = 7.0kT$ shown in fig. 3(a) (the solid curve) was unfolded using eq. (24). Figure 6 shows the results, the curve labelled I is the input distribution and curve 0 is the unfolded output distribution.

Finally, a supplementary procedure to the Primak method for obtaining the activation energy distribution is possible. For very broad distributions it leads to the same result, however, it may be used to extend the analysis into the region of FWHM as small as a few kT .

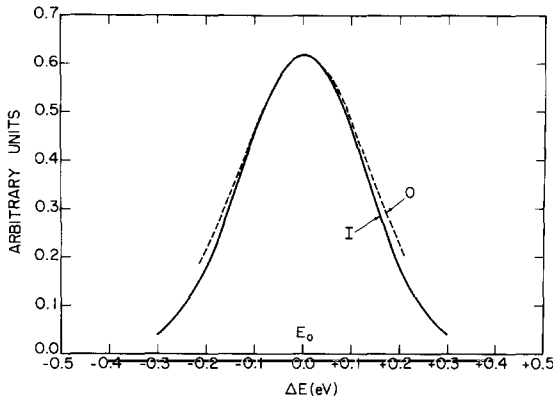


Fig. 6. The unfolding of the relaxation curve shown in fig. 3(a) for the Gaussian activation distribution (solid line) using the Primak approximation of eq. (24). The solid line curve labelled I is the input distribution, the dashed line curve labelled O is the unfolded resulting output.

By making use of eq. (5) $\alpha = se^{-E/kT}$, eq. (19) may be written as a function of α :

$$\frac{dn}{dt} = -kT \int_0^s \eta(\alpha, 0) e^{-\alpha t} d\alpha. \quad (26)$$

The upper limit of the integral in eq. (26) may be replaced by infinity since the frequency factor s is usually very large (e.g. $10^9 < s < 10^{14} \text{ s}^{-1}$). With this substitution, the observed TL intensity is kT times the Laplace transform of $\eta(\alpha, 0)$. It follows that $\eta(\alpha, 0)$ is the inverse Laplace transform of $-(1/kT) \cdot (dn/dt)$.

Generating the inverse Laplace transform directly from experimental data is a formidable task. However, if the data can first be fitted with an analytic function the task is mathematically manageable, particularly if the function should be one of those appearing in a table of Laplace "pairs" [17].

It had been noted by Medlin [18] that for broad activation energy distributions of the Gaussian form, it is possible to cast the TL relaxation rate into the form:

$$I = -dn/dt = I_0(1 + bt)^{-\mu} \quad (27)$$

with μ and b constants.

When intended to simply extend the divergent t^{-1} relaxation rate, μ is close to unity and $bt > 1$ over most of the observed range of bt . This form for TL relaxation is observed to hold for some

experiments with even larger values of μ and a wider range of values for bt including $bt < 1$.

The function given in eq. (27) does appear as one of the tabulated pair of Laplace functions and yields a distribution:

$$\eta(\alpha, 0) = I_0 \alpha^{\mu-1} e^{-\alpha/b} / kT b^\mu \Gamma(\mu), \quad (28)$$

where $\Gamma(\mu)$ is the gamma function of μ . Equation (5) relating α and E converts eq. (28) into an energy distribution.

In cases where the distribution width FWHM is greater than several kT , the Primak approximation stated in eqs. (24) and (25) should also be valid. This approximation leads to the result:

$$\eta(\alpha, 0) = I_0 / \alpha kT (1 + b/\alpha)^\mu. \quad (29)$$

The two equations, eq. (28) and (29), are in fact quite similar for $b/\alpha > 1$ (hence $\alpha/b < 1$) and for μ nearly unity. Expanding eq. (28) in a power series of α/b yields:

$$\eta(\alpha, 0) = \frac{I_0 (\alpha/b)^\mu}{\alpha kT \Gamma(\mu)} \cdot \left(1 - \frac{\alpha}{b} + \frac{\alpha^2}{2b^2} + \dots \right); \quad (30)$$

while the expansion of eq. (29) gives closely the same result:

$$\eta(\alpha, 0) = \frac{I_0 (\alpha/b)^\mu}{\alpha kT} \times \left(1 - \mu \frac{\alpha}{b} + \frac{\mu(\mu+1)}{2} \frac{\alpha^2}{b^2} + \dots \right), \quad (31)$$

note $\Gamma(1.25) = 0.906$.

For a sum of closely spaced very narrow activation energy levels generally giving only a single unresolved glow peak the isothermal relaxation rate:

$$I = \sum_i \alpha_i n_i(0) e^{-\alpha_i t} \quad (32)$$

relates to the distribution:

$$\eta(\alpha, 0) = \sum_i n_i(0) \delta(\alpha - \alpha_i), \quad (33)$$

where $\delta(\alpha - \alpha_i)$ is the delta function locating the energy of the level designated by the index i and the corresponding total level occupancy is $n_i(0)$ at $t = 0$.

4. Discussion and conclusions

It is found possible to normalize the stretched exponential relaxation function to an appropriate decay function based on a Gaussian activation energy distribution using first order kinetics. By working at the normalization point $x = \alpha_0 t = t/\tau_0 = 1$ it is possible to associate a particular value of y with each value of ζ . Such paired relaxation curves are found to be nearly indistinguishable in the range $0.1 < x < 10$. Comparison of the two activation energy distributions reveals that this close congruence in relaxation rates over a range of about a factor 100 in time is due primarily to the similarity in values of the FWHM of the two distributions resulting from the normalization procedure.

It is necessary to have short-time relaxation rate data, t values as low as $x = 0.01$, in order to observe the presence of the striking low energy tail of the distribution corresponding to the stretched exponential, a tail which is not significantly present in the Gaussian distribution. These data may be difficult to obtain experimentally for TL due to the finite time it takes to bring the phosphor sample to the isothermal observation temperature from room temperature. For example, in the $\text{CaF}_2:\text{Mn}$ isothermal TL experiments at least 25 s were required to reach substantial thermal equilibrium in going from room temperature to 230 °C. This corresponds to $x = 0.02$. The need for storage at a low temperature after irradiation to allow fading to go to completion prevents irradiation at the isothermal elevated temperature which would be a means for reducing this "heat up" time.

To observe the difference in the high energy region of the two activation energy distributions requires reaching values of $x > 10$. In the analysis of TL data presented here it was assumed that there is no retrapping present. If retrapping were present it would be expected to become increasingly significant for values of $x > 1$. This is due to the fact that retrapping effectively transfers some electrons from trap sites having shallower activation energies to trap sites having deeper activation energies. These electrons in turn are finally released at times greater than that corresponding to $x = 1$, a time when the window function is span-

ning the energy region near E_0 . It should be noted that the $\text{CaF}_2:\text{Mn}$ phosphor appears to have some retrapping present in its TL kinetics behavior [6].

In view of the above difficulties it is likely that TL isothermal relaxation rate experiments will mostly be sensitive to the activation energy distribution width and will not be able to distinguish definitively between various possible bell-shaped energy distributions in their entirety.

The most successful experimental program for determining the important TL characteristics: s , E_0 , FWHM, and the retrapping factor $\beta N/\alpha n_0$ for a kinetics model of the type shown in fig. 1, is to obtain both a TL glow curve and an isothermal relaxation measurement [6]. The initial rise method applied to the glow curve yields values for s and E_0 and hence $\alpha_0 = 1/t_0$. The relaxation rate data in the time range $0.1 < x = \alpha_0 t < 10$ should yield a reasonable value for the FWHM.

If retrapping is not too severe the following rules pertain in the range $0.1 < x < 10$ and possibly beyond:

- (i) for $\zeta < 0.2$ (FWHM > 0.5 eV)* an inverse time dependence prevails for the relaxation rate;
- (ii) for $0.2 < \zeta < 0.4$ (0.5 eV $>$ FWHM > 0.25 eV) a relaxation rate results obeying a function of the type $I_0(1 + bt)^{-\mu}$ with μ near 1 and I_0 the initial rate at $t = 0$;
- (iii) for $0.4 < \zeta < 0.99$ (0.25 eV $>$ FWHM > 0.02 eV) only the transitional behavior results for the relaxation rate, requiring tabulated or numerically computed unfolding;
- (iv) For $0.99 < \zeta < 1$ (0.02 eV $>$ FWHM > 0) an exponentially decaying relaxation rate follows.

Relaxation rate experiments indicating time dependent behavior of the types (i) or (ii) above should yield a reasonable measure of the activation energy distribution near E_0 using the Primak analysis contained in eqs. (24) and (25). At the narrower end of the distribution range given in (ii) and in those cases where at least in the critical region $0.1 < x < 10$, the relaxation rate is ade-

* Corresponding values of y may be found in table 1 or by use of eq. (15).

quately matched by the function in eq. (27), the data for cases with FWHM widths as small as only a few kT may be sufficiently characterized by the distribution given in eq. (28). At the broader end of the range given in (ii) the Primak method is to be preferred since it treats the observed data directly.

There are potentially important problems with the theoretical aspects of the development pursued above. Even for the simple kinetic model of fig. 1 the treatment of n_c and dn_c/dt is questionable. For example, near $t = 0$ (albeit masked by experimental difficulties) dn_c/dt is of the same order of magnitude as dn/dt and hence not negligible as must be assumed for the application of either relaxation function of eq. (14) to the TL data. The TL observed is given by dm/dt not dn/dt . In general $dm/dt = dn/dt + dn_c/dt$ and $m = n + n_c$. To properly determine dm/dt , no approximations concerning n_c should be made, rather the relevant differential equations should be solved exactly.

It should be noted that the use of differential equations for the time rates of change of n , m , and n_c obscure any stochastic processes that might be present. This is particularly true for the transport of the electrons (n_c) in the conduction band as they move across the sample prior to arriving at a recombination center. The usual treatment for the luminescent capture of the conduction electrons (n_c) is to associate a capture cross section σ with each trapped hole m and use the average velocity \bar{v}_c for the sea (gas) of conduction electrons to yield the bimolecular reaction rate:

$$dm/dt = -\bar{v}_c \sigma m n_c = -\gamma m n_c.$$

The very likely presence of retrapping should be added to the model of fig. 1 [11].

To address these questions, an extensive numerical program has been begun to study the kinetic model of fig. 1 with retrapping added. The activation energy distribution is divided into R sections with adjustable electron occupancies at $t = 0$. The $R + 2$ resulting coupled differential

equations are solved simultaneously to give all the relevant quantities (e.g. dm/dt , n_c , dn_c/dt , n_R) as the kinetics parameters are varied. At present only the program with $R = 5$ is running. The more desirable program with $R = 7$ should be running soon. Additional experimental work is also contemplated.

Acknowledgements

This work was funded in part by the NSF: BNS8911758 and the Naval Surface Warfare Center: N6092189M4352. We are indebted to V.K. Mathur and J. Silverman for many useful discussions during the course of this research.

References

- [1] R. Kohlrausch, Pogg. Ann. 91 (1854) 179.
- [2] F. Kohlrausch, Pogg. Ann. 119 (1863) 337.
- [3] A. Plonka, Time-Dependent Reactivity of Species in Condensed Media, Lecture Notes in Chemistry 40 (Springer, New York, 1986).
- [4] H.B. Rosenstock, Phys. Rev. 187 (1969) 1166.
- [5] J. Noolandi, Phys. Rev. B 16 (1977) 4474.
- [6] J.T. Bendler and M.F. Shlesinger, Macro. Mol. 18 (1985) 591.
- [7] J. Klafter and M.F. Shlesinger, Proc. Natl. Acad. Sci. USA 83 (1986) 848.
- [8] R. Visocekas, M. Ouchene, and B. Gallois, Nucl. Instr. and Meth. 214 (1983) 553.
- [9] P.A. Clark and R.H. Templer, Archaeometry 30 (1988) 19.
- [10] W.F. Hornyak and A.D. Franklin, J. Lumin. 42 (1988) 89.
- [11] W.F. Hornyak and A.D. Franklin, Nucl. Tracks Radiat. Meas. 14 (1988) 81.
- [12] R. Chen, W.F. Hornyak and W.K. Mathur, Phys. Rev. D, to be published.
- [13] K.W. Wagner, Ann. Phys. 40 (1913) 817.
- [14] E. Jahnke and F. Emde, Table of Functions 38 (Dover, New York, 1943).
- [15] G.H. Weiss, Amer. Sci. 71 (1983) 65.
- [16] W. Primak, J. Appl. Phys. 31 (1960) 1524.
- [17] I.S. Gradshteyn and I.M. Ryzhik, Table of Integrals, Series and Products (Academic, New York, 1980).
- [18] W.L., Medlin, Phys. Rev. 123 (1961) 502.